

Research Paper

Purification and Characterization of Gigantoxin-4, a New Actinoporin from the Sea Anemone *Stichodactyla Gigantea*

Bo Hu*, Wei Guo*, Liang-hua Wang*, Jian-guang Wang, Xiao-yu Liu✉, Bing-hua Jiao✉

Department of Biochemistry and Molecular Biology, Second Military Medical University, Shanghai 200433, China

* These authors made equal contributions to this work.

✉ Corresponding author: Department of Biochemistry and Molecular Biology, Second Military Medical University, Shanghai 200433, China. Tel: 86-21-81870965; Fax: 86-21-65334344. E-mail: liuxiaoyu8888@msn.com (Xiao-yu Liu), jiaobh@live.cn (Bing-hua Jiao).

© Ivyspring International Publisher. This is an open-access article distributed under the terms of the Creative Commons License (<http://creativecommons.org/licenses/by-nc-nd/3.0/>). Reproduction is permitted for personal, noncommercial use, provided that the article is in whole, unmodified, and properly cited.

Received: 2011.04.04; Accepted: 2011.05.30; Published: 2011.06.07

Abstract

A new Cytolysin, termed as Gigantoxin-4, was isolated from the sea anemone *Stichodactyla gigantea* and found to be highly homologous with Cytolysin-3 (HMg III) from *Heteractis magnifica*, RTX-A from *Radianthus macrodactylus*, and Sticholysin-1 (St I) and Sticholysin-2 (St II) from *Stichodactyla helianthus* (homology 82%, 86%, 82% and 86% respectively). Its 20 N-terminal residues were identified and the full-length cDNA sequence was obtained by reverse transcription-polymerase chain reaction (RT-PCR). Multiple sequence alignments with other Cytolysins of the actinoporin family clearly indicated that Gigantoxin-4 belongs to this protein family. SDS-PAGE electrophoresis showed that this new actinoporin had a molecular mass of about 19 kDa, and possessed a high hemolytic activity to human erythrocytes ($HA_{50} = 40$ ng/ml), which was inhibited by pre-incubation with sphingomyelin (SM) or SM-cholesterol mixtures. Our *in vivo* experiments showed that Gigantoxin-4 had wide toxicity to the rat cardiovascular system and the respiratory system. A concentration of 30 µg/kg Gigantoxin-4, i.v. produced a positive inotropic effect on the rat heart although final cardiovascular failure was inevitable, and 60 µg/kg Gigantoxin-4 caused respiratory arrest rapidly resulting in rat death. HE staining indicated pathological changes in various organs and tissues after i.v. administration of Gigantoxin-4.

Key words: Sea anemone, *Stichodactyla gigantea*, Actinoporin, Sphingomyelin, *in vivo*

INTRODUCTION

Sea anemones are rich sources of biologically active peptides and proteins, including neurotoxins [1], enzymes [2, 3] and cytolysins [4, 5]. Actinoporins are 20 kDa cytolytic proteins that interact with sphingomyelin in cellular and artificial membranes found in sea anemone [6]. Equinatoxins from *Actinia equina* [7] and sticholysins from *Stichodactyla helianthus* [8] are two of the most studied representatives of the actinoporin family, a class of eukaryotic pore-forming

toxins (PFTs) found in sea anemones. The molecular mechanism of pore formation has been considered a multi-step process that involves recognition of membrane sphingomyelin, firm binding to the membrane accompanied by the transfer of the N-terminal region to the lipid-water interface and finally pore formation after oligomerisation of 3-4 monomers with accompanying pore formation [6, 9]. Cytolysin-1 and Cytolysin-2 (HMg I and II) [10], and Cytolysin-3 [11]

belong to the family of Cytolysins from the sea anemone *H. magnifica*. Recent research in 52 cloned HMg gene sequences showed that HMgs are encoded by a multigene family whose members are highly homologous to each other [12]. Some sea anemone toxins, including cytolysins and neurotoxins, have been investigated for their putative cardiotoxic actions [13] and anticancer effects [14].

An epidermal growth factor (EGF)-like toxin (gigantoxin I) and two sodium channel toxins (gigantoxins II and III), previously isolated from the sea anemone *Stichodactyla gigantea* [15], Gigantoxin I is the first example of EGF-like toxins of natural origin [16]. The present work reported the isolation and characterization of a new actinoporin toxin from *S. gigantea*, whose cDNA sequences were confirmed by RT-PCR. In addition, we also tried to clarify interactions between lipid vesicles and Gigantoxin-4. The toxic effect of Gigantoxin-4 *in vivo* was also studied by directly injecting the Gigantoxin-4 in anaesthetized Sprague-Dawley (SD) rats.

MATERIALS AND METHODS

Animals and venom collection

Specimens of *S. gigantea* were collected from the South China Sea. The tentacles of live animals were cut into pieces and then thoroughly freeze dried. A total volume of 20 ml cold deionized H₂O was added to 5 g tentacle pieces. The suspension was homogenized with a blender for 15 min at 4°C and centrifuged for 20 min at 27,000 ×g at 4°C. The supernatant was stored for future use. Part of the sample was quickly frozen in liquid nitrogen for total RNA preparation and then stored at -75°C.

Purification of Gigantoxin-4 from *Stichodactyla gigantea*

One milliliter reconstituted crude extract was purified with a filter (pore diameter 0.45 μm). The filtrate was applied to a Hitrap Capto S cation exchange column (0.7×2.5 cm, GE, USA) connected to an ÄKTA purifier 100 System (GE Healthcare, Sweden). The column for chromatography was eluted with a step NaCl gradient, where elution buffer A was 50mM ammonium acetate (pH 5.6), and elution buffer B was 1 M NaCl, 50 mM ammonium acetate (pH 5.6). The elution started with 0% buffer B, with its proportion raised to 11%, 21%, 30% and 100% after every 5 ml of elution volume at a flow rate of 1 ml/min. The eluted peak was monitored simultaneously at a wavelength of 215 and 280 nm. Peaks showing the high hemolytic activity were collected and lyophilized.

The hemolytic fractions were further purified by gel chromatography. A total of 2 ml concentrated protein solution was applied to a HiLoad 16/60 Superdex 75 prep grade size-exclusion column (60 × 1.6 cm, GE, USA). The column for chromatography was equilibrated and eluted with 150 mM ammonium acetate (pH 5.1) at a flow rate of 1 ml/min. Eluted peaks were monitored simultaneously at a wavelength of 215 and 280 nm. Peaks showing the high hemolytic activity were collected and lyophilized.

The protein concentration of the purified Gigantoxin-4 was determined by the ultraviolet spectrophotometric method. The separation of each fraction was monitored by SDS-PAGE.

Mass spectrometry analysis and N-terminal amino acid sequence determination

The Nano-LC MS/MS experiment was performed in the proteomics laboratory of Fudan University School of Medicine (Shanghai, China) using an HPLC system composed of two LC-20AD nano-flow LC pumps, an SIL-20 AC auto-sampler and an LC-20AB micro-flow LC pump (all Shimadzu, Tokyo, Japan) connected to an LTQ-Orbitrap mass spectrometer (ThermoFisher, San Jose, CA). MGF files were analyzed using Mascot 2.2.07 against the NCBI nr database 2010 Sep release.

The N-terminal amino acid sequence analysis was performed as described by Bellomio et al [17]. SDS-PAGE protein bands (about 19 kDa) corresponding to the hemolytic peaks were transferred to a polyvinylidene fluoride (PVDF) membrane, and were then excised to have their 20 N-terminal residues sequenced by the Edman degradation method with a PROCISE™492cLC (ABI, USA).

Cloning and determination of the sequence

Total RNA was obtained from a single specimen of *S. gigantea* following the manufacturer's instructions of RNAiso Plus (TaKaRa, Japan) and was used as a template for synthesis and amplification of cDNAs coding for actinoporins using a RevertAid First Strand cDNA Synthesis Kit (Fermentas, USA) following the manufacturer's instructions. Peak 2' showed a high similarity and identity with Cytolysin-3 using BLASTP according to mass spectrometry and N-terminal amino acid sequencing results. Thus, the complete cds of gIII (GenBank: AF170706.1) were used to design primers. The forward primer (CGTCTCATCGTCTTATTT) and the reverse primer (TGTCTTCTTATTAGCGTG) were used in RT-PCR. cDNAs with a size about 630 base pairs were purified from PCR products and sent to Invitrogen Corporation to determine the sequence.

Hemolytic activity (HA) and inhibition of the hemolytic activity of Gigantoxin-4

The hemolytic activity was assayed as described by de Oliveira et al [18]. An erythrocyte suspension was prepared using fresh human red blood cells and washed with phosphate-buffered saline (PBS) until the supernatant was clear. Erythrocytes were resuspended in the same buffer to a final erythrocyte concentration of 0.5%. The erythrocyte suspension was incubated with various concentrations of Gigantoxin-4 at 37°C for 30 min and then centrifuged at 3,000 g for 5 min to precipitate both intact erythrocytes and ghosts. Optical density of the supernatant was measured using a microplate reader (Bio-Rad, USA) at 420 nm. Background or total cell hemolysis was evaluated by incubation of erythrocytes with PBS or 0.5% Triton X-100 in PBS. The percentage of hemolysis was calculated as follows: %hemolysis = $[(Abs_{\text{sample}} - Abs_{\text{PBS}}) / (Abs_{\text{Triton}} - Abs_{\text{PBS}})] \times 100$.

In another experiment, the erythrocyte suspension was incubated with Gigantoxin-4 (0.08 µg/ml) at 37°C for 10, 20, 30, 40, 50 and 60 min, respectively. The hemolytic activity was assayed by the same method and observed with a laser scanning confocal microscope (LeicaCTS SP2).

Small unilamellar vesicles (SUV) were prepared as described [19] and used for the experiment on inhibition of the hemolytic activity. SUV of egg phosphatidylcholine (PC), sphingomyelin (SM), SM: cholesterol (Cho) 1:1, SM: PC 1:1 and SM: Cho: PC 1:1:1 (molar ratios) were incubated with Gigantoxin-4 (0.1 µg/ml to promote 100% hemolysis) at different lipid concentrations, and the remaining HA was assayed as previously described.

Physicochemical factors influence on HA of Gigantoxin-4

Gigantoxin-4 (0.1 µg/ml) was incubated for 20 min at temperatures from 20°C to 80°C, and preserved at 25°C for 6, 12, 24 and 36 h to assess the influence of preservation time on Gigantoxin-4 toxicity. In another experiment, Gigantoxin-4 was freeze-thawed for 5, 10 and 20 cycles. After completing these experiments, toxins were submitted for hemolytic assay.

Permeabilization of LUV

Large unilamellar vesicles (LUVs) were prepared as previously described [20]. The permeabilizing effect of Gigantoxin-4 on LUV was determined by measuring the fluorescence of released calcein with a fluorescence microplate reader (Biotek synergy2, USA) with excitation and emission wavelengths set at 485 nm and 535 nm [21]. Gigantoxin-4, at various concentrations in a vesicle buffer, was dispensed in a

multiwell microplate, and then in an appropriate amount of calcein-loaded LUV (0.1 M final concentration), the volume totaling 200 µl. After mixing the vesicles and the toxin, fluorescence intensity increased due to the release of calcein. Maximum release was always obtained by adding 0.5% Triton X-100 (final concentration) and provided the fluorescence value F_{max} . The percentage of release R (%) was calculated as follows: $R (\%) = (F_{\text{sample}} - F_{\text{in}}) / (F_{\text{max}} - F_{\text{in}}) \times 100$, where F_{in} and F_{sample} represent the initial and the sample (steady-state) value of fluorescence before and after toxin addition.

General surgical procedures and *in vivo* hemodynamics

Male SD rats weighing 280-330 g were supplied by the Laboratory Animal Center of the Second Military Medical University in Shanghai, China. All animal experiments were approved by the Ethics Committee of said university. The general surgical procedures were similar to those described previously [22].

Male SD rats were anaesthetized with pentobarbital sodium (60 mg/kg i.p.) and the trachea was cannulated to facilitate mechanical ventilation. A catheter was inserted into the left femoral artery for recording blood pressure (BP) by connecting it to a BP transducer. Another catheter was inserted into the left femoral vein for intravenous administration of Gigantoxin-4. The mean arterial pressure (MAP) was derived from the BP pulse. Left ventricular pressure (LVP) and heart rate (HR) were measured through a Millar BP catheter (SPR-524, Millar Instruments Inc, US), which was introduced through the right carotid artery into the left ventricular cavity and connected to another BP transducer. The first derivative of LVP (dP/dt_{max} , dP/dt_{min}), an index of cardiac systolic and diastolic function, was derived from differentiating the signal of LVP using an electronic differentiator. A Powerlab/8SP ADInstruments System (Pty.Ltd. Castel Hill, Australia) was used to monitor and record changes of dP/dt_{max} , dP/dt_{min} , MAP and HR.

Analysis of activities of liver and heart damage-related enzymes

At 30 and 60 min of Gigantoxin-4 injection (30µg/kg i.v.), blood samples were collected in heparinized tubes. Liver and heart damage-related enzymes including alanine aminotransferase (ALT), aspartate aminotransferase (AST), lactate dehydrogenase (LDH), creatine kinase (CK) and MB isoenzyme of creatine kinase (CK-MB) were determined using an automatic biochemical analyzer (Hitachi 917, Japan).

Histopathological analysis

After treatment with Gigantoxin-4 (30 $\mu\text{g}/\text{kg}$ i.v.) for 60 min, the heart, lung, liver and kidney were collected from SD rats, fixed in 10% paraffin formaldehyde, sliced to 6-mm sections, hematoxylin and eosin (HE) stained, and then examined under a light microscope (100 \times magnification).

Statistical analysis

Values were expressed as mean \pm SD. Statistical analysis was performed either by Student's *t* test for paired data or unpaired data. Differences were considered to be significant at **p* < 0.05, ***p* < 0.01.

RESULTS

Purification of Gigantoxin-4

Cation-exchange on Capto S column of water solution of the crude extract of *S. gigantea* presented four peaks, of which peak 1 and 2 were hemolytic (Fig. 1A). Then peak 1 was pooled, lyophilized and

applied onto a Superdex 75 column and peak 1' with hemolytic activity was obtained (Fig. 1B). In the same way, peak 2 was applied onto the Superdex 75 column and peak 2' with hemolytic activity was obtained (Fig. 1C). SDS-PAGE electrophoresis showed that peak 1' and 2' had an apparent molecular mass of about 19 kDa (Fig. 1E).

Mass spectrometry and N-terminal amino acid sequencing

The N-terminal amino acid sequences of the purified peak 1' and 2' were both determined as SASAVAGTIIIEGASLTFQILDKV (amino acids from 1 to 22). The Nano-LC MS/MS experiment revealed two internal peptide sequences: SGTTDVILP EFVFNQKALL YSGR; G IMTSAGEAK (Fig. 2A). The sequences of N-terminal amino acid and peptide as assayed by MS/MS were almost identical to that of Cytolysin-3 reported by Wang et al [12]. We named peaks 2' as Gigantoxin-4, all the researches below focused on peak 2'.

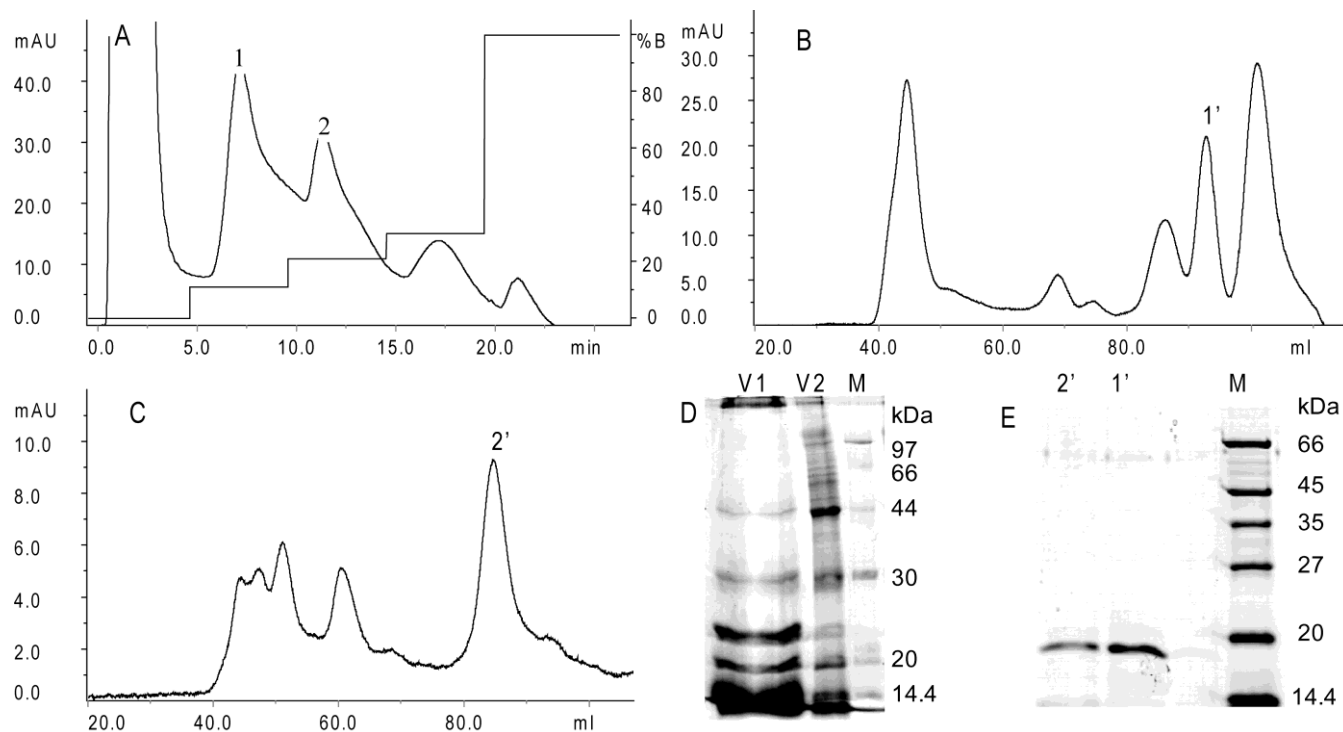


Fig. 1. Purification of Gigantoxin-4. (A) Cation-exchange chromatography on Hitrap Capto S (0.7 \times 2.5 cm, GE, USA) using an ÄKTA purifier 100 System (GE, USA). 1 ml crude extract was applied to the column, which was eluted with a gradient of 11%, 21%, 30% and 100% NaCl (1.0 M) in 50 mM ammonium acetate buffer (pH 5.6) at a flow rate of 1 ml/min. Peak 1 and 2 show the high hemolytic activity collected. (B) Gel-filtration chromatography. 2 ml of the concentrated peak 1 protein solution was applied to the Superdex 75 column (1.6 \times 60 cm, GE, USA), which was eluted with 150 mM ammonium acetate buffer (pH 5.1) with a flow rate of 1 ml/min. (C) Gel-filtration chromatography. A concentrated sample of peak 2 was applied to the Superdex 75 column. (D) SDS-PAGE analysis of mucus exudates (V1) and crude extract (V2) from *S. gigantea*. (E) SDS-PAGE analysis of fractions collected after Gel-filtration chromatography. (M) Marker, (1') peak 1', (2') peak 2'.

```

1      ATCGCTGTGCAATCTGGAAAGAAATTCCAAGGCAGAAAAAGGACAAGAAGAGTGCTTCA
1      I A V Q S G K K F Q G R K E D K K S A S
61     GCAGTCGCTGGCACAAT TATCGAAGGGCAAGTCTAACTTTCCAAATCCTTGACAAAAGTA
21     A V A G T I I E G A S L T F O I L D K V
121    CTCACAGA ACTTGGTAA TGTG TCTCGGAAGATTGCTATCGGATCGAC AACGAGTCAGGA
41     L T E L G N V S R K I A I G I D N E S G
181    GGGTCATG GACAGCAAT GAATGCATA TTCCGTTCTGGTACTACAGACGTCATTCTACCA
61     G S W T A M N A Y F R S G T T D V I L P
241    GAGTTTGTCCCAAACAA TAAAGCGCTACTCTACAGCGGTCGGAAGGACACAGGCCCTGTT
81     E F V P N N K A L L Y S G R K D T G P V
301    ACAACGGGCGCTGTGGGTGCCCTTGCCTAT TACATGAGCGATGGAACACTCTTGCCGTT
101    T T G A V G A L A Y Y M S D G N T L A V
361    ATGTT CAGCGTTCCCTTTGACTACAACCTGTACAGCAACTGGTGGGATGTCAGAGTCTAT
121    M F S V P F D Y N L Y S N W W D V R V Y
421    AGTGGGAA GAGGAGAGCCGACCAAAA GATGTACGAAGACCTCTATAATGGCTCTCCATTT
141    S G K R R A D Q K M Y E D L Y N G S P F
481    AAAGGGGA CAATGGATGGCACCAGAA GAATCTTGATATGGACTGAGGATGAAGGGAATC
161    K G D N G W H Q K N L G Y G L R M K G I
541    ATGACAAGTGCTGGCGAAGCAAACTGCAATT AAGATTTCACGCTAA
181    M T S A G E A K L Q I K I S R *

```

A

Sticholysin-2ALAGTIIAGASITTFQVLD	18
Actinoporin Or-GGATTAGAALGFNVHQ	15
Cytolysin-3	MNRLIVLFLIVTMICATIIVPSREELEDQKEYKRS.AALAGTIIIEGASLGFQILD	54
Cytolysin RTX-AALAGAIAGASITTFQILD	18
Equinatoxin-2	MSRLIIVFIVVTMICSATALPSKKIIDEEDEDEKRSADVAGAVIDGASLSFDILK	55
Gigantoxin-4IAVQSGKKFQGRKEDKKSASAVAGTIIIEGASITTFQILD	38
Sticholysin-1SELACTIIDGASITTFEVLDD	19
Consensus	g i g a l f	

Sticholysin-2	KVLEELGKVSRKIAVIGIDNESGGTWTALNAYFRSGTTDVLPEFVVENTKALLYSG	73
Actinoporin Or-G	TVLKALGQVSRKIAIGVDNESGGTWTALNAYFRSGTTDVLPEFVFNQKALLYSG	70
Cytolysin-3	KVIGELGKVSRKIAVIGVDNESGGSWTALNAYFRSGTTDVLPEFVFNQKALLYSG	109
Cytolysin RTX-A	KVLAELGQVSRKIAIGIDNESGGSWTAMNAYFRSGTTDVLPEFVFNQKALLYSG	73
Equinatoxin-2	TVLEALGNVSRKIAVIGVDNESGKTWTALNTYFRSGTSDIVLPHKVPHGKALLYNG	110
Gigantoxin-4	KVITELGNVSRKIAIGIDNESGGSWTAMNAYFRSGTTDVLPEFVFNQKALLYSG	93
Sticholysin-1	KVIGELGKVSRKIAVIGIDNESGGTWTALNAYFRSGTTDVLPEVVENTKALLYSG	74
Consensus	vl lg v r k i a g d n e s g w t a l n a y f r s g t d v l p e v v e n t k a l l y g	

Sticholysin-2	RKDTGPVATGAVAAAFAYYMSNGNTLGVMFVSPFDYNNWYSNWWVDVKIYSGKRRADQ	128
Actinoporin Or-G	OKDTGPVATGAVGVLAYYMSDGNLGVMFVSPFDYNNLYSNWWVDVKVYRGRRRADQ	125
Cytolysin-3	RKDTGPVATGAVAAAFAYYMSNGHTLGVMFVSPFDYNNFYSNWWVDVKVYSGKRRADQ	164
Cytolysin RTX-A	RKNRGPDTTGAVALAYYMSNGNTLGVMFVSPFDYNNLYSNWWVDVKVYSGKRRADQ	128
Equinatoxin-2	OKDRGPVATGAVGVLAYLMSDGNLAVLFSVPYDYNWYSNWWNVRIYKGRRRADQ	165
Gigantoxin-4	RKDTGPVTTGAVGALAYYMSDGNLAVMFVSPFDYNNLYSNWWVDVRYSGKRRADQ	148
Sticholysin-1	RKSSGPVATGAVAAAFAYYMSNGNTLGVMFVSPFDYNNWYSNWWVDVKIYSGKRRADQ	129
Consensus	k gp tgav ay ms g tl v fsvp dyn ysnww v y g rradq	

Sticholysin-2	GMYEDLYYGN.FYRGDNGWHEKNLGYGLRMKGIIMTSAGEAKMQIKISR	175
Actinoporin Or-G	AMYEGLLYGI.FYGGDNGWHARKLGYGLKGRGFMKSSAQSI LEIHVTK	172
Cytolysin-3	GMYEDMYIGN.FYRGDNGWHQKNLGYGLRMKGIIMTSAGEAIIQIRISR	211
Cytolysin RTX-A	AMYEDLYYSN.FYRGDNGWHQKNLGYGLKMKGIIMTSAGEAIMEIRISR	175
Equinatoxin-2	RMYEELYNLS.FFRGDNGWHTRNLGYGLKSRGFMNSSGHAILEIHVSK	213
Gigantoxin-4	KMYEDLYNGS.FFKGDNGWHQKNLGYGLRMKGIIMTSAGEAKLQIKISR	195
Sticholysin-1	GMYEDMYIGN.FYRGDNGWYQKNLGYGLRMKGIIMTSAGEAKMQIKISR	176
Consensus	mye p gdngw lgygl g m s i	

B

Fig. 2. cDNA sequence and multiple sequence alignment of Gigantoxin-4. (A) cDNA sequence of Gigantoxin-4. The corresponding amino acid sequence is shown in boldface. The sequences of N-terminal amino acid and peptide as assayed by MS/MS are underlined. **(B)** Multiple sequence alignment of actinoporins. Alignment was performed with CLUSTLW in the Uniprot Knowledgebase. Identical residues are shown on a gray background.

cDNA cloning and multiple sequence alignment of Gigantoxin-4

cDNA of Gigantoxin-4 revealed an open reading frame of 195 amino acids with the ATC stop coding at position 588 (Fig. 2A). The deduced protein had a predicted signal peptide composed of the first 17 amino acids. A molecular mass of 19 kDa was predicted for the putative mature protein, which matched our SDS-PAGE results. A sequence similarity search in the GenBank database using BLASTN and BLASTP programs indicated that Gigantoxin-4 should belong to the actinoporin family. When aligned with the known actinoporins, the deduced complete amino acid sequences of Gigantoxin-4 showed a high similarity and identity with Cytolysin-3 from *H. magnifica* (82%), RTX-A from *R. macrodactylus* (86%), Sticholysin-1 (82%) and Sticholysin-2 (86%) from *S. helianthus*, Or-G from *Oulactis orientalis orientalis* (72%) [23], and Equinatoxin-2 from *A. equina* (65%) (Fig. 2B).

In vitro activity, inhibition and influencing factors of Gigantoxin-4-induced hemolysis

The concentration of Gigantoxin-4 that lysed 50% erythrocytes was 45 ng/ml (Fig. 4A), which was

similar to that of St I and St II ($HA_{50} \approx 30-45$ ng/ml) obtained by Lanio et al [8]. Gigantoxin-4 induced 100% hemolysis at the concentration of 80 ng/ml.

After Gigantoxin-4 (80 ng/ml) treatment, erythrocytes showed a series of changes with a gradual emergence of deformation and ultimate death within 40 min (Fig. 3A). Hemolytic effects of Gigantoxin-4 on erythrocytes were observed under the prescribed vision with a laser scanning confocal microscope (Fig. 3B - Fig. 3E).

The hemolytic activity of Gigantoxin-4 was inhibited significantly by preincubation with SUV composed of SM/Cho or SM/Cho/PC, and almost completely bereaved at a low concentration of 3 μ g/ml (Fig. 4B), while no significant inhibitory effect of PC lipids on the hemolytic activity of Gigantoxin-4 was observed even at a high concentration of 1 mg/ml. The hemolytic activity of Gigantoxin-4 was also almost entirely inhibited by SUV composed of SM/PC at a concentration of 0.1 mg/ml, but SUV composed of pure SM only caused a 20% decrease in the hemolytic activity of Gigantoxin-4 at the same concentration (Fig. 4B).

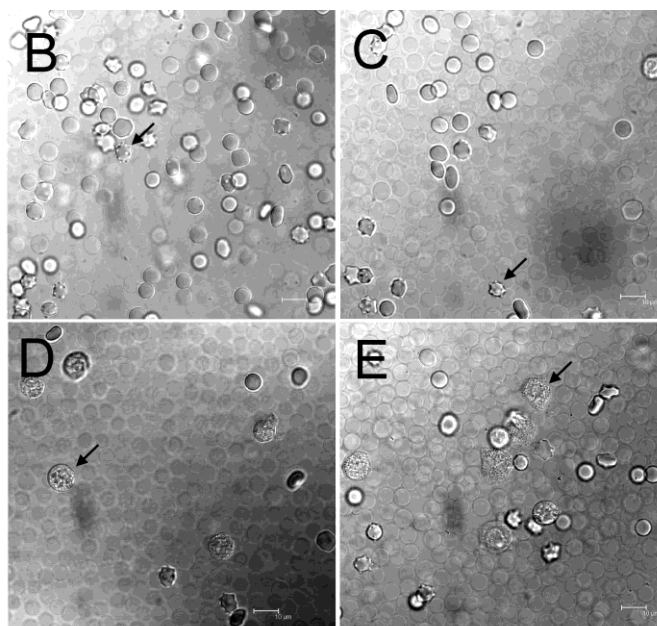
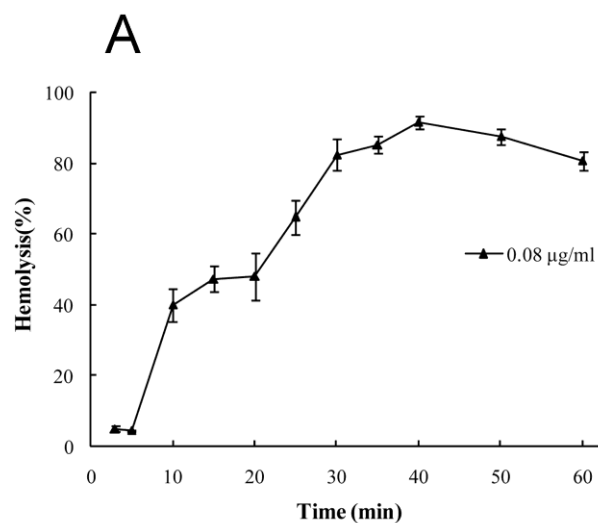


Fig. 3. Hemolytic activity of Gigantoxin-4. (A) Time-dependent changes *in vitro* of Gigantoxin-4-induced hemolysis. The series of changes (indicated by the arrow) with a gradual emergence of deformation and ultimate death of erythrocytes were observed with laser scanning confocal microscope (1000 \times magnification) after (B) 10 min, (C) 20 min, (D) 30 min and (E) 40 min. Scale bar corresponds to 10 μ m.

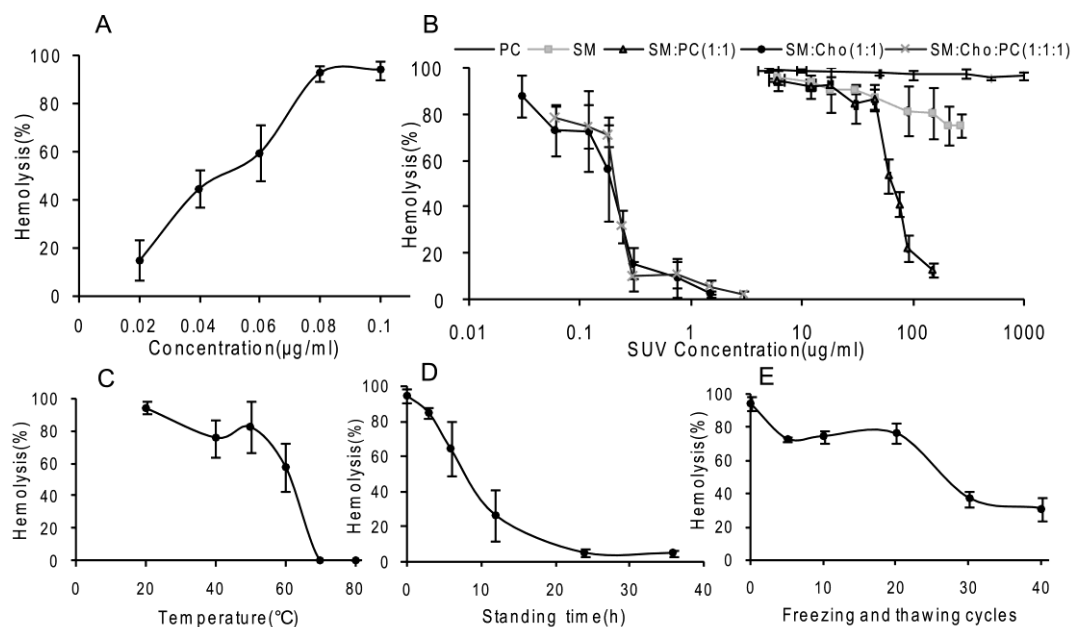


Fig. 4. *In vitro* activity, inhibition and influencing factors of Gigantoxin-4-induced hemolysis. (A) Concentration dependence. The concentration of Gigantoxin-4 to lyse 50% erythrocytes is 45ng/ml. (B) Inhibition of Gigantoxin-4-induced hemolysis by SUV. Gigantoxin-4 (0.1µg/ml) was preincubated (30 min at 37°C) with an appropriate amount of SUV. The mixture was diluted with erythrocyte buffer to the desired vesicle concentration and incubated for 30 min at 37°C. Hemolysis was monitored at 420 nm. Each result is the mean value of three experiments. (C) Influence of temperature on the hemolytic activity of Gigantoxin-4. (D) Influence of standing time on the hemolytic activity of Gigantoxin-4 at room temperature. (E) Influence of freeze-thaw cycles on the hemolytic activity of Gigantoxin-4. All data are expressed as mean \pm SD (n = 5).

Temperature was a very important factor influencing the stability of Gigantoxin-4 *in vitro*. After 20-min incubation at 20°C, 40°C, 50°C and 60°C, the hemolytic ability of Gigantoxin-4 gradually decreased. When it was heated to 70°C and 80°C, the hemolytic activity of Gigantoxin-4 was almost completely lost (Fig. 4C). Repeated freeze-thaw cycles also inactivated Gigantoxin-4. Although 25 freeze-drying cycles caused a 25% loss of the hemolytic activity, there was still 40% hemolytic activity remaining after 40 freeze-drying cycles (Fig. 4D). In addition, the hemolytic activity of Gigantoxin-4 gradually decreased in response to prolonged standing time at room temperature, and 24 h later the protein was almost completely degraded (Fig. 4E). We also found that there were no obvious difference if adding protease inhibitors (10 mM PMSF and EDTA) or not (data was not shown). Therefore, we got the conclusion that the activity loss of Gigantoxin-4 is not due to the contamination with proteases but the high temperature or solution condition resulting in the protein denaturation.

Permeabilizing effect on LUV

Our result showed that a calcein leak was de-

tectable when LUV composed of SM: Cho: PC (1:1:1 molar ratio) was used. The percentage of calcein release increased with the Gigantoxin-4 concentration increasing. However, almost no calcein was detectable when LUV composed of pure PC was used (Fig. 5).

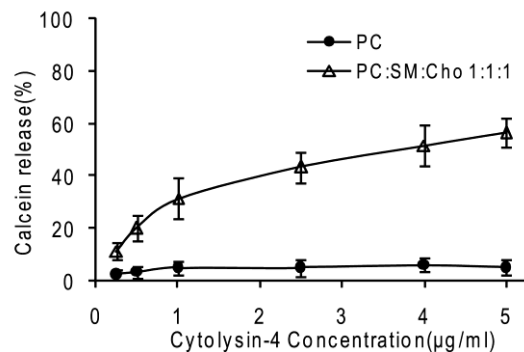


Fig. 5. Permeabilization of LUV. It was determined by measuring the fluorescence of released calcein with a fluorescence microplate reader (Biotek synergy2, USA). The excitation wavelength was 485 nm and emission wavelength was set at 535 nm. 200 µl Gigantoxin-4 of different concentrations dissolved in vesicle buffer (140 mM NaCl, 20 mM Tris, 1 mM EDTA, pH 7.5) was added into each well, and calcein release was monitored. Each value is expressed as mean \pm SD (n = 5).

Dose and time dependent changes *in vivo* left ventricle (LV) function induced by Gigantoxin-4 in SD rats

A total of 10 rats were used to determine whether injection of Gigantoxin-4 (30 $\mu\text{g}/\text{kg}$ and 60 $\mu\text{g}/\text{kg}$, i.v.) influenced LV function. Gigantoxin-4 administration (60 $\mu\text{g}/\text{kg}$, i.v.) evoked a transient hypotensive and bradycardic effect when pressor response was observed. However, fatal cardiovascular collapse ensued within 3 min, causing rat death (Fig. 6). A mild and transient decline in BP was also observed at a low dose of 30 $\mu\text{g}/\text{kg}$, followed by a gradual increase in the following 20 min (Fig. 6). In addition, dP/dt , MBP and HR kept increasing for about 25 min and then gradually decreased within 30-60 min (data not shown). Interestingly, decreased hemodynamics induced by Gigantoxin-4 (60 $\mu\text{g}/\text{kg}$, i.v.) could be gradually restored and even increased significantly when the rat was connected to the breathing machine on time, extending the life span of the rat by tens of minutes to hours. However, the rat died immediately when the breathing machine was withdrawn.

Effects of Gigantoxin-4 on liver and heart damage-related enzymes

As shown in Fig. 7A, the liver damage-related enzymes ALT and AST were significantly increased 60 min after Gigantoxin-4 injection (30 $\mu\text{g}/\text{kg}$ i.v.) compared with those of the control group. In addition,

LDH, CK and CK-MB were significantly increased after 30-min Gigantoxin-4 administration (Fig. 7B).

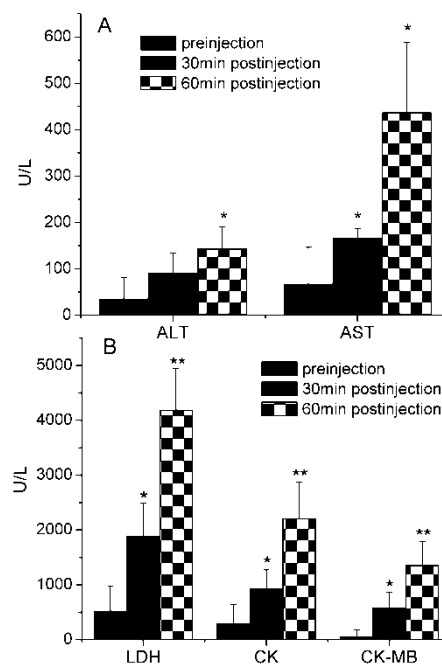


Fig. 7. Effects of Gigantoxin-4 at 30 $\mu\text{g}/\text{kg}$ i.v. on ALT, AST, LDH, CK and CK-MB. All the results were expressed as mean \pm SD (n=6). Significant difference from the respective preinjection value was expressed as * $p < 0.05$, ** $p < 0.01$.

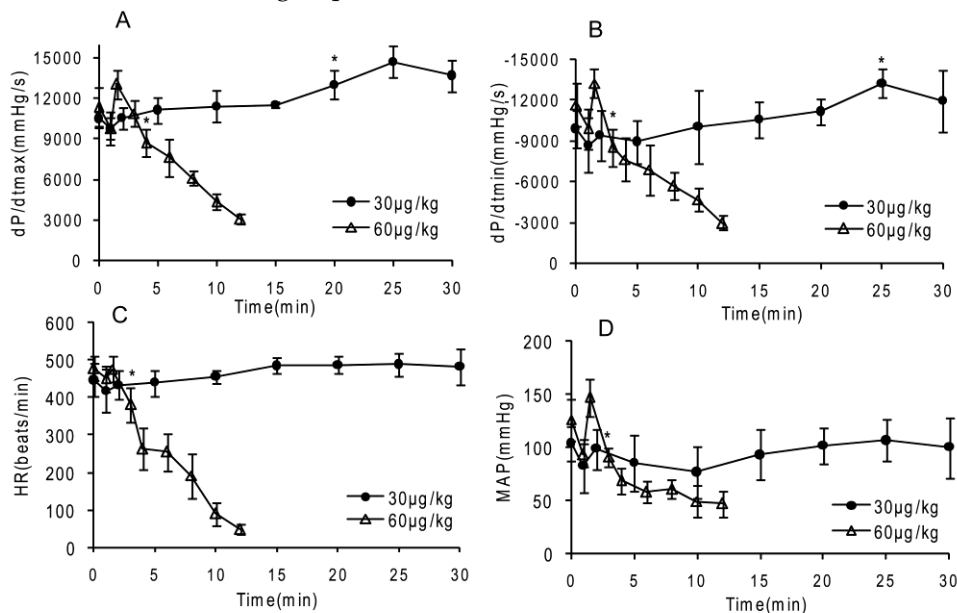


Fig. 6. Dose and time-dependent changes *in vivo* LV function induced by Gigantoxin-4 (30 $\mu\text{g}/\text{kg}$ and 60 $\mu\text{g}/\text{kg}$, i.v.) in SD rats. $\pm dP/dt$ = slope of LVP, HR= heart rate, MAP= mean femoral arterial pressure. Control data were preinjection value (0 min), and data are mean \pm SD (n=6). Significant difference from the respective preinjection value was expressed as * $p < 0.05$.

Histopathological analysis

Damage to important tissues of the rats (Fig. 8) was also evaluated 60 min after Gigantoxin-4 (30 µg/kg i.v.) administration. HE-staining showed acute pulmonary congestion, interstitial edema, alveolar wall thickening and slight infiltration of tissue fluid into alveolar space in the lung (Fig. 8E). The myocardial tissue was congested, with sporadic necrosis (Fig.

8F). Acute congestion and multiple focal necroses were observed in the liver (Fig. 8G). Sporadic hemorrhage and hyaline casts were observed in the kidney (Fig. 8H). These toxic effects of Gigantoxin-4 on organs were similar to those observed in tentacle-only extract (TOE) venom from jellyfish *Cyanea capillata* [24].

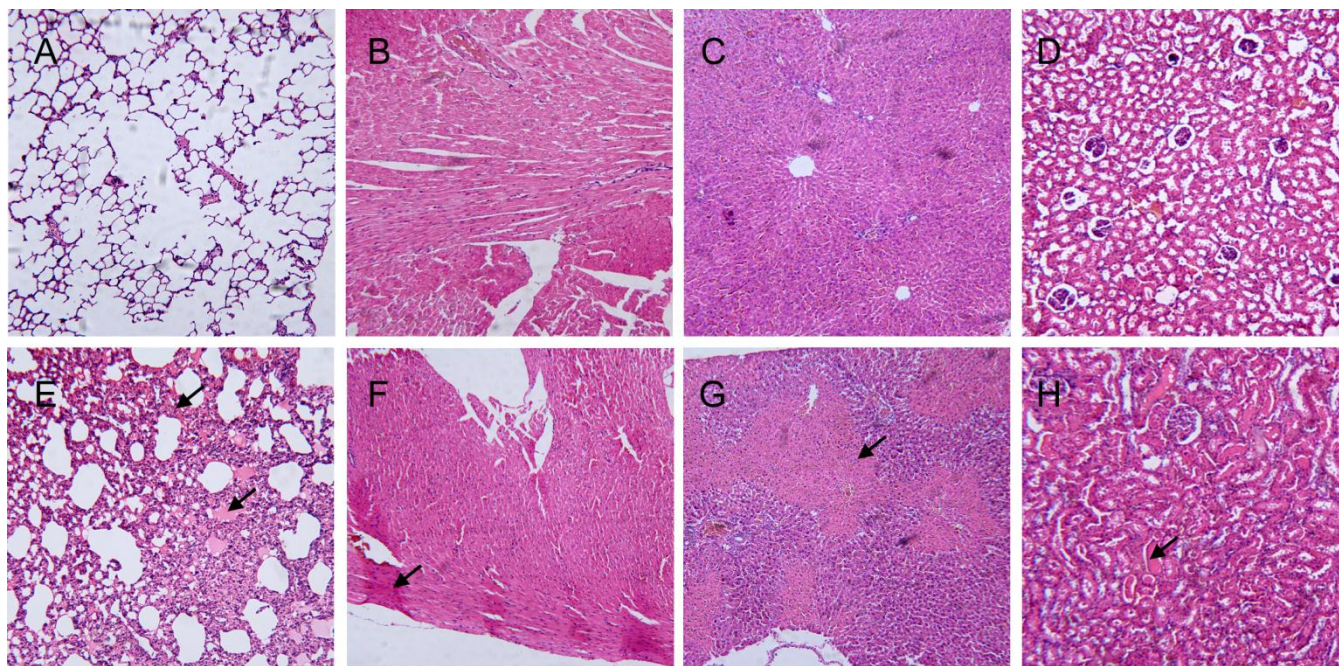


Fig. 8. Histopathological analysis of the lung, heart, liver and kidney of SD rats 60 min after Gigantoxin-4 administration (30 µg/kg i.v.) (100× magnification). (A) Normal pulmonary tissue. (B) Normal heart tissue. (C) Normal liver tissue. (D) Normal kidney tissue. (E) Acute congestion was present in the lung (indicated by the arrow). (F) Sporadic necrosis was present in the heart. (indicated by the arrow). (G) Multiple focal necroses were present in the liver (indicated by the arrow). (H) Sporadic hemorrhage was present in the kidney (indicated by the arrow).

DISCUSSION

The present study characterized the structure and bioactivities of a new cytolyisin isolated from the sea anemone *Stichodactyla gigantea*, termed as Gigantoxin-4, identified its 20 N-terminal residues, and obtained the full-length cDNA sequence. A sequence similarity search in the GenBank indicated that Gigantoxin-4 should belong to the actinoporin family due to the high sequence similarity to Cytolysin-3 (82%), Sticholysin-1 (82%), Sticholysin-2 (86%) and RTX-A (86%).

It was reported that actinoporin could make pores in cellular, lipid or artificial membranes, which could be formed efficiently, especially when cell membranes contained sphingomyelin [25-28]. Pore

formation on the cell surface may increase membrane permeability or cause leakage of cell contents, leading to cell death. Our work confirmed that Gigantoxin-4 induced lysis of erythrocytes ($HA_{50}=40$ ng/ml) and leakage of calcein wrapped in LUV, indicating that the target of Gigantoxin-4 was the cell membrane. We also found that the various components of the lipid membrane showed different potential interactions with Gigantoxin-4. SUV composed of pure PC showed no significant effect on hemolytic activity. The hemolytic activity of Gigantoxin-4 could be inhibited more rapidly and significantly by SUV composed of SM/Cho/PC as compared with SUV composed of pure SM. Similar data was obtained by a permeabilization experiment of LUV. No leakage of

calcein was observed when LUV composed of pure PC was used. However, a calcein leak was detectable when LUV composed of SM: Cho: PC was used, indicating that Cytosin-4 had a high affinity to LUV composed of SM and Cho. Although our results are not completely consistent with the reports of other researchers, one point is identical: when SM is one component of the cell membrane, it will be affected by the cytolytic effect of actinoporins.

Another important finding of the present study is that administration of a high concentration of Gigantoxin-4 (60 µg/kg, i.v.) caused respiratory arrest, which might be the primary factor causing death of the rat. Histological analysis also confirmed that the lung was the most seriously injured organ after Gigantoxin-4 administration. The lung has been considered the predominant site of marginated neutrophil pool [29]. The hemolysis induced by Gigantoxin-4 caused the leakage of cell contents, thus stimulating activation of neutrophils. Activated neutrophils appear to play a central role in the development of acute lung injury in most cases [30]. Therefore, our study gives an important reference for the design of therapeutic strategies of sea anemone stings. By comparison, rats can live tens of minutes to hours after injecting low-dose Gigantoxin-4 (30 µg/kg, i.v.), although final cardiovascular failure was inevitable. The hemolysis induced by Gigantoxin-4 also maybe cause hyperkalemia, the most common cause of heart failure due to the massive hemolysis in the blood of the rat. Biochemical analysis showed that plasma levels of liver and heart related enzymes were increased significantly, indicating that the toxic effect of Gigantoxin-4 was systemic. Similar results were found in EqT II from *A. equina*, causing a drop in the perfusion rate, decrease in LVP, arrhythmia and increased LDH release [13]. Our further research will focus on how to block or mitigate the damage to cells and organs induced by Gigantoxin-4.

ACKNOWLEDGEMENT

We thank Samantha Weber for careful reading of the manuscript.

CONFLICTS OF INTEREST

The authors declare that there are no conflicts of interest.

REFERENCES

- Norton R.S. Structure and structure-function relationships of sea anemone proteins that interact with the sodium channel. *Toxicon*, 1991. 29(9): 1051-84.
- Lotan A, Fishman L, and Zlotkin E. Toxin compartmentation and delivery in the Cnidaria: the nematocyst's tubule as a multiheaded poisonous arrow. *J Exp Zool*, 1996. 275(6): 444-51.
- Linder R and Bernheimer A.W. Effect on sphingomyelin-containing liposomes of phospholipase D from *Corynebacterium ovis* and the cytolysin from *Stichodactyla helianthus*. *Biochim Biophys Acta*, 1978. 530(2): 236-46.
- Kem W.R and Dunn B.M. Separation and characterization of four different amino acid sequence variants of a sea anemone (*Stichodactyla helianthus*) protein cytolysin. *Toxicon*, 1988. 26(11): 997-1008.
- Klyshko E.V, et al. Isolation, properties and partial amino acid sequence of a new actinoporin from the sea anemone *Radianthus macrodactylus*. *Toxicon*, 2004. 44(3): 315-24.
- Kristan K.C, et al. Molecular mechanism of pore formation by actinoporins. *Toxicon*, 2009. 54(8): 1125-34.
- Macek P and Lebez D. Isolation and characterization of three lethal and hemolytic toxins from the sea anemone *Actinia equina* L. *Toxicon*, 1988. 26(5): 441-51.
- Lanio M.E, et al. Purification and characterization of two hemolysins from *Stichodactyla helianthus*. *Toxicon*, 2001. 39(2-3): 187-94.
- Bakrac B and Anderluh G. Molecular mechanism of sphingomyelin-specific membrane binding and pore formation by actinoporins. *Adv Exp Med Biol*, 2010. 677: 106-15.
- Khoo K.S, et al. Purification and partial characterization of two cytolysins from a tropical sea anemone, *Heteractis magnifica*. *Toxicon*, 1993. 31(12): 1567-79.
- Wang Y, Chua K.L, and Khoo H.E. A new cytolysin from the sea anemone, *Heteractis magnifica*: isolation, cDNA cloning and functional expression. *Biochim Biophys Acta*, 2000. 1478(1): 9-18.
- Wang Y, et al. A multigene family of *Heteractis magnifica* lysins (HMgs). *Toxicon*, 2008. 51(8): 1374-82.
- Bunc M, et al. Effects of equinatoxin II from *Actinia equina* (L.) on isolated rat heart: the role of direct cardiotoxic effects in equinatoxin II lethality. *Toxicon*, 1999. 37(1): 109-23.
- Fedorov S, et al. The anticancer effects of actinoporin RTX-A from the sea anemone *Heteractis crispa* (= *Radianthus macrodactylus*). *Toxicon*, 2010. 55(4): 811-7.
- Honma T, et al. Molecular cloning of an epidermal growth factor-like toxin and two sodium channel toxins from the sea anemone *Stichodactyla gigantea*. *Biochim Biophys Acta*, 2003. 1652(2): 103-6.
- Shiomi K, et al. An epidermal growth factor-like toxin and two sodium channel toxins from the sea anemone *Stichodactyla gigantea*. *Toxicon*, 2003. 41(2): 229-36.
- Bellomio A, et al. Purification, cloning and characterization of fragaceatoxin C, a novel actinoporin from the sea anemone *Actinia fragacea*. *Toxicon*, 2009. 54(6): 869-80.
- de Oliveira J.S, et al. Caissarolysin I (Bcs I), a new hemolytic toxin from the Brazilian sea anemone *Bunodosoma caissarum*: purification and biological characterization. *Biochim Biophys Acta*, 2006. 1760(3): 453-61.
- Razpotnik A, et al. A new cytolytic protein from the sea anemone *Urticina crassicornis* that binds to cholesterol- and sphingomyelin-rich membranes. *Toxicon*, 2009. 53(7-8): 762-9.
- Tejuca M, et al. Mechanism of membrane permeabilization by sticholysin I, a cytolysin isolated from the venom of the sea anemone *Stichodactyla helianthus*. *Biochemistry*, 1996. 35(47): 14947-57.
- Valcarcel C.A, et al. Effects of lipid composition on membrane permeabilization by sticholysin and II I, two cytolysins of the sea anemone *Stichodactyla helianthus*. *Biophys J*, 2001. 80(6): 2761-74.
- Wang L.G, et al. Comparative study of NMDA and AMPA/kainate receptors involved in cardiovascular inhibition produced by imidazoline-like drugs in anaesthetized rats. *Exp Physiol*, 2007. 92(5): 849-58.

23. Il'ina A.P, et al. [Actinoporins from the Sea of Japan anemone *Oulactis orientalis*: isolation and partial characterization]. *Bioorg Khim*, 2005. 31(1): 39-48.
24. Xiao L, et al. The lethality of tentacle-only extract from jellyfish *Cyanea capillata* is primarily attributed to cardiotoxicity in anaesthetized SD rats. *Toxicon*, 2010. 55(4): 838-45.
25. Alvarez C, et al. Sticholysins, two pore-forming toxins produced by the Caribbean Sea anemone *Stichodactyla helianthus*: their interaction with membranes. *Toxicon*, 2009. 54(8): 1135-47.
26. Schon P, et al. Equinatoxin II permeabilizing activity depends on the presence of sphingomyelin and lipid phase coexistence. *Biophys J*, 2008. 95(2): 691-8.
27. Drechsler A, et al. Effect of lipid on the conformation of the N-terminal region of equinatoxin II: a synchrotron radiation circular dichroism spectroscopic study. *Eur Biophys J*, 2009. 39(1): 121-7.
28. Miles A.J, et al. The effects of lipids on the structure of the eukaryotic cytolytic equinatoxin II: a synchrotron radiation circular dichroism spectroscopic study. *Biochim Biophys Acta*, 2008. 1778(10): 2091-6.
29. Hogg J.C and Doerschuk C.M. Leukocyte traffic in the lung. *Annu Rev Physiol*, 1995. 57: 97-114.
30. Abraham E. Neutrophils and acute lung injury. *Crit Care Med*, 2003. 31(4 Suppl): S195-9.